Cross sections relevant to gamma-ray astronomy: Alpha-particle-induced reactions on ^{12}C, ^{14}N, and ^{16}O nuclei

P. Dyer*
Heavy Ion Laboratory, Michigan State University, East Lansing, Michigan 48824
and Physics Division, Los Alamos National Laboratory, Los Alamos, New Mexico 87545

D. Bodansky, Donald D. Leach, Eric B. Norman,† and Alan G. Seamster‡
Nuclear Physics Laboratory, University of Washington, Seattle, Washington 98195
(Received 28 June 1985)

Gamma-ray production cross sections have been measured for the gamma-ray lines most strongly excited in the alpha-particle bombardments of ^{12}C, ^{14}N, and ^{16}O for alpha-particle energies from threshold to 27 MeV. Tabulations of cross sections averaged over alpha-particle energy bins of 1 MeV are provided for calculations relevant to gamma-ray line astronomy. Relevance to analysis of spectra acquired with gamma-ray spectrometers in space is discussed.

I. INTRODUCTION

Energetic charged particles are produced in a broad range of astrophysical sources. These include solar flares, regions of star formation, black holes, and the galactic center. Astrophysical observations of the γ rays produced in the nuclear reactions induced by these particles have the potential for providing information on the energies, directions, and abundances of these particles and on the abundances of the nuclei in the ambient medium. The main developments have been reviewed by Ramaty and Lingenfelter.[1] Most of the unambiguous observations of γ-ray lines have thus far been limited to solar flares,[2] although some lines have been seen from the galactic center[3] and, more recently, the special object SS433.[4] Interpretation of such data, as well as possible future observations of other sources or of richer spectra, requires knowledge of γ-ray production cross sections for proton- and α-particle-induced reactions on abundant nuclei.

Here we present cross sections for the most prominent γ rays produced by α particles on ^{12}C, ^{14}N, and ^{16}O nuclei, at incident energies from threshold to 27 MeV. Cross sections for proton-induced reactions on these nuclei and on four heavier nuclei, ^{20}Ne, ^{24}Mg, ^{28}Si, and ^{56}Fe, have been presented in an earlier paper,[5] henceforth called (I), and those for α-particle-induced reactions on the four heavier nuclei, plus ^{27}Al, in a second paper,[6] henceforth called (II). Alpha-particle-induced reactions may in some cases be as important as proton-induced reactions, particularly for soft astrophysical spectra, as has been pointed out in (II).

The experimental procedures used in these measurements are outlined in Sec. II. Only the techniques for yield extraction at the higher energies (where the lines are significantly Doppler broadened) are different from those of our previous measurements. The results are presented in Sec. III and are discussed in Sec. IV.

II. EXPERIMENTAL METHOD

A. General

The experimental setup for these measurements was the same as that used for the studies of proton-induced reactions (I). Thin solid or gas targets were bombarded with α-particle beams of energies from threshold to 27 MeV from the University of Washington tandem Van de Graaff accelerator. Beam currents ranged from 5 to 100 nA and were typically 10 nA. Gamma rays were detected by two Ge(Li) detectors, one 79 cm^3 and one 50 cm^3. In the case of carbon- and nitrogen-target runs, these detec-

TABLE I. Targets used for gamma-ray cross section measurements. The indicated thickness is the stopping power thickness, as seen by the beam, and includes isotopic and elemental impurities. All targets were natural. (The indicated C target angle is the angle between the beam direction and the normal to the target foil.)

Target nucleus	Thickness[a] (mg/cm^2)	Angle (deg)	E_α (MeV)
Carbon	0.18±0.01	20, 45, 60	7.7–11.0
	0.51±0.03	45, 60	11.3–16.0
	2.02±0.15	20, 60	16.7–27.0
Nitrogen	0.50		7.4–9.8
	0.76		9.8–14.0
	1.52		14.0–27.0
Oxygen	0.58		10.2–13.8
	1.73		14.0–27.0

[a]For the gas targets the thickness uncertainty was 5%.

tors were placed at 109.9° and 30.6° [where $P_4(\cos\theta)=0$], so that total cross sections could be determined from the two differential cross section measurements, as γ-ray multipolarities were 2 or less. In the case of oxygen-target runs, where the 6.130-MeV γ ray has a multipolarity of 3 and the decaying state has spin 3, at least three differential cross section measurements at special angles would be required to determine the total cross section. Here we measured the complete angular distribution by acquiring data at four angles (26°, 48.8°, 90°, and 104°). Efficiencies of the Ge(Li) detectors were measured for γ-ray energies below 4 MeV with calibrated radioactive sources and for γ-ray energies of 4.439 and 6.130 MeV by comparison of proton and γ-ray yields in the $^{12}C(p,p'\gamma)^{12}C$ and $^{16}O(p,p'\gamma)^{16}O$ reactions (I). Efficiencies at 6.917 and 7.117 MeV were determined by extrapolation of our lower energy results, guided in part by other studies of Ge(Li) detector efficiencies as a function of γ-ray energy.[7]

The targets used and their thicknesses are listed in Table I. Carbon data were acquired with foils of natural carbon. The carbon foil thicknesses were determined from measurements with an alpha-particle source, comparisons of count ratios for the several targets, comparisons to counts with gas targets, and comparisons to measurements of known proton scattering cross sections. The quoted uncertainties reflect the internal consistency between the results of these several methods. The total thicknesses of these targets, used to calculate E_α (labora-

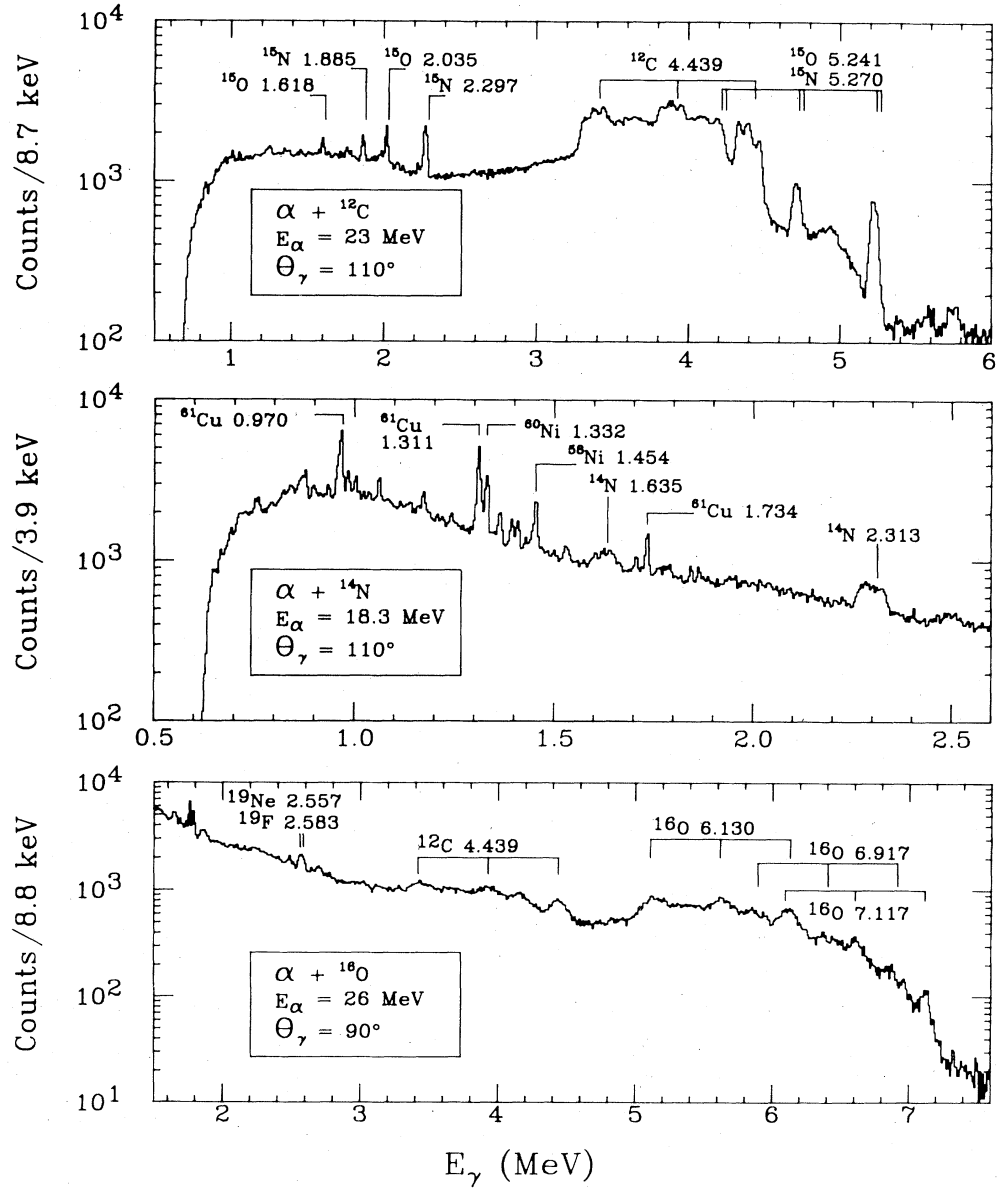

FIG. 1. Typical γ-ray spectra, in 79 cm^3 Ge(Li) detector, for α-particle bombardment of C, N, and O targets. Prominent peaks are identified by residual nucleus and transition energy. The vertical marker lines are located at energies calculated for zero Doppler shift.

tory energy) at the target center, exceed the ^{12}C thicknesses by about 3%, of which 1% is attributable to ^{13}C and 2% to ^{16}O; the ^{16}O thickness was estimated from earlier (p,p') measurements and from measurements of 6.130 MeV γ-ray yields from the carbon targets.

Nitrogen and oxygen data were acquired with a 2.54-cm diameter gas cell (I) containing high purity, natural gases. The thicknesses were measured by monitoring the pressure in the cell, assuming the gas remained close to room temperature. Nickel entrance and exit foils on the gas cell were 0.905 mg/cm^2 for incident energies below 14 MeV and 1.80 mg/cm^2 above 14 MeV. [In (II), the latter thickness had been taken to be 1.718 mg/cm^2, introducing a small error in the calculated central energies (e.g., about 0.02 MeV at $E_\alpha = 16$ MeV)].

Data were acquired using conventional electronics. Beam energies were stepped in units of average energy loss in the target up to 20 MeV, after which larger (1 MeV) steps were taken. Typical spectra are shown in Fig. 1.

Doppler shifts, which are expected to be relatively large in the present case of α particles incident upon light nuclei, are clearly visible in the ^{12}C and ^{14}N spectra of Fig. 1, where at 110° the observed peaks lie at energies below the transition energies. In addition, there is a substantial Doppler broadening of the peak widths, with the attendant complications in peak area extraction, discussed below in Sec. II B. Nevertheless, despite the noticeable kinematic effects, no appreciable error is introduced in the calculation of the total cross sections, largely because data is taken both forward and backward of 90°. More specifically, in checks over a broad span of incident energies, the present calculated total cross sections, based on laboratory differential cross sections at only a few angles, agree within about 2% with total cross sections calculated from fuller angular distributions, extending from 30° to 150°.

B. Peak area extraction by line shape fitting

In the analyses of the data for incident protons (I) and for incident α particles on nuclei with $A \geq 20$ (II), the total yield was obtained from the difference between the total number of counts in the γ-ray photopeak and a background found by interpolation of the count rates below and above the peak. However, for the present case, i.e., for α particles incident on light nuclei, the large Doppler broadening often leads to low peak-to-background ratios and to excessive uncertainties in the determination of peak areas using this method (method A). The problem of peak area extraction is compounded in the case of ^{16}O, due to the overlap of the peaks arising from the 6.130-, 6.917-, and 7.117-MeV γ rays. To obtain more accurate yield determinations in cases where the peaks were poorly defined, a line shape fitting method (method B) was employed. The specific choices of method and a comparison between the results from method A and B are discussed in Sec. II C. In the remainder of this section, details of method B are described.

In method B, each Doppler-broadened γ-ray peak is viewed as being the sum of contributions from a set of narrow peaks whose central energies span the width of the observed peak. The standard shape of the narrow peaks is taken to be the experimental shape found in (p,p') reactions with low-energy protons (I). The central positions and amplitudes of the narrow peaks are treated as adjustable parameters, determined by a best fit to the observed shape of the broad peak. In a compromise between limitations of computer time and refinement of fit, eight narrow peaks were used to fit each of the broad peaks. This method directly addresses the problem of subtracting the contributions from the single and double escape peaks and Compton tails of higher energy γ-ray lines (assuming these too are fit using a similar procedure) as well as of subtracting counts within a broad peak which arise from the intrusion of the Compton tail of high-energy components of that peak into the low-energy region of the same peak.

A set of starting parameters for the fit was determined using the derivation of Kolata *et al.*[8] for the shape of a Doppler broadened γ-ray line:

$$\frac{dY_\gamma}{dE}(E) = \sum \left[\int_0^{\theta_R^{\max}} \frac{\sigma(\theta_R) S(\theta_R,E) \Omega(\theta_R,E) \sin\theta_R \, d\theta_R}{\{[E_0\beta(\theta_R)\sin\theta_R \sin\theta_D]^2 - [E - E_0\beta(\theta_R)\cos\theta_R \cos\theta_D]^2\}^{1/2}} \right], \quad (1)$$

where E_0 is the transition energy, E is the difference between the observed γ-ray energy E_γ and E_0 ($E = E_\gamma - E_0$), θ_D is the γ-ray angle of emission, θ_R and ϕ_R are the polar and azimuthal angles of the recoiling nucleus, $\sigma(\theta_R)$ is the differential cross section for producing recoils at θ_R, $\beta(\theta_R)$ is the velocity (in units of c) of the recoil, and $Y_\gamma(E)$ is the relative number of γ rays with energy shift E detected at θ_D. (All angles are measured relative to the incident beam direction.) The quantity $\Omega(\theta_R,E)$ corresponds to the angular distribution of γ rays, where the angular dependence is expressed in terms of E, rather than θ_R, via the Doppler formula:

$$E = E_0\beta(\theta_R)(\cos\theta_R\cos\theta_D + \sin\theta_R\sin\phi_R\sin\theta_D) . \quad (2)$$

This function $\Omega(\theta_R,E)$ can be calculated once the population of magnetic substates of the recoiling nucleus is known. The function $S(\theta_R,E)$ is 0 or 1 depending on whether the recoil cone angle contributes to the γ-ray yield. The summation sign indicates that the integration is to be performed for both kinematic branches of $\beta(\theta_R)$.

To generate the set of starting parameters for a nonlinear least squares fit to the data, a spectrum is calculated from Eq. (1), assuming that the recoil angular distributions are isotropic in the center-of-mass system and that only the $m = 0$ magnetic sublevel of the excited state is populated. (The final result is not sensitive to these assumptions, as only starting parameters for the fit are being determined.) The kinematically allowed peak region is

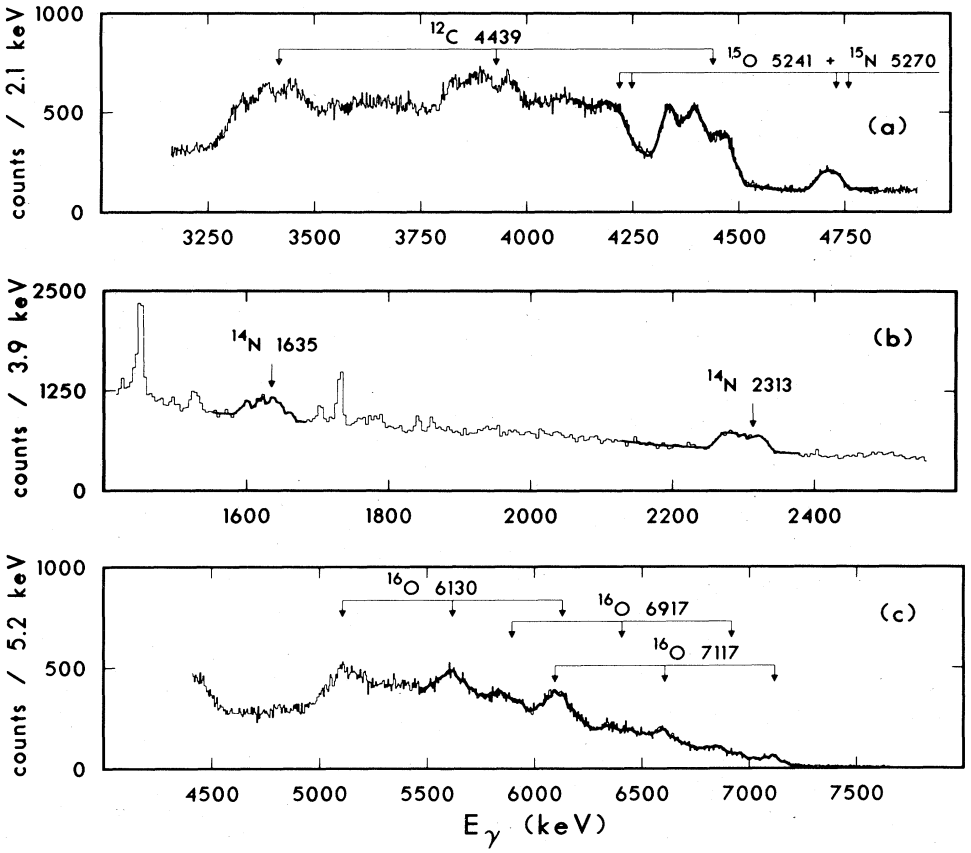

FIG. 2. Comparison between observed peak shapes and those calculated using the method of Sec. II B for α-particle bombardment of C, N, and O targets [(a), (b), and (c), respectively]. Peaks are identified by residual nucleus and transition energy. The light lines correspond to the observed spectra and the dark lines to the calculated fits. For each target, θ_γ and E_α are the same as in Fig. 1.

divided into eight parts, the centers of which become the starting-parameter peak positions. In the subsequent fit, these positions are constrained to vary less than 10, 20, or 26 keV for ^{12}C, ^{14}N, or ^{16}O, respectively. This gives us some confidence that if the final fit is good, no other γ rays contribute significantly to the spectrum (barring very close transition energies). The starting parameters for the eight peak amplitudes are also taken from Eq. (1), using an overall normalization obtained from a crude peak area analysis.

The shape of each of the eight narrow peaks is taken numerically from data acquired (for each detector) with low-energy incident protons. (For the ^{14}N 1.635-MeV line, 1.634-MeV γ rays from p+^{20}Ne data were used.) Compton tails are thus treated correctly and, in the case of the ^{16}O analysis, single and double escape peaks are correctly incorporated along with the photopeaks. For an isolated γ ray, the number of variable parameters is normally 17 or 18: eight peak amplitudes, eight peak positions (constrained in range of variation), and one or two background parameters (constant plus possible slope). Typical fits to the spectra are shown in Fig. 2.

In the case of fits to the ^{12}C 4.439-MeV lines, peak sums were obtained from a 17-parameter fit to the photopeak region (isolated γ ray) for alpha particle energies below 19.4 MeV. At higher energies, the double escape peak from γ rays of 5.270 MeV [from the ^{12}C(α,p)^{15}N reaction] and 5.241 MeV [from the ^{12}C(α,n)^{15}O reaction] interfered with a simple extraction of counts. A 33-parameter fit (16 amplitudes + 16 peak positions + constant background) was made to a region of the spectrum including the 4.439-MeV photopeak and the single and double escape peaks of the 5.241-MeV and 5.270-MeV doublet (the 5-MeV line shapes taken to be the same as the 4.439-MeV line shape).

For ^{14}N 1.635-MeV line fits, 17 parameters were varied. The background was taken to be linear, with its amplitude fixed above the peak by the background level, and its slope allowed to vary. At the higher energies, contributions from the Ni foil were significant. The Ni peaks were included in the fit; then, using data acquired with an empty cell, the Ni contribution was subtracted. The ^{14}N 2.313-MeV line fits were straightforward. Eighteen parameters were varied (including two parameters describing a linear background). No Ni peak subtraction was required, and there was no evidence of other nearby γ-ray lines.

The fitting procedure was most complex in the case of the ^{16}O spectra at α-particle energies above 12 MeV, because a separation of yields from overlapping 6.130-6.917-, and 7.117-MeV γ rays was required. A 50-parameter fit was considered intractable. Therefore, with starting parameters determined from Eq. (1), a 17-parameter fit (fit 1) of the 7.117-MeV photopeak region

was made. Next the region of the 6.917- and 7.117-MeV photopeaks and single-escape peaks was fit (fit 2), with the eight 7.117-MeV peak positions fixed at the values determined in fit 1. Fit 2 thus dealt with 25 variable parameters. Starting parameters for the 6.917-MeV peak were determined from Eq. (1); those for the 7.117-MeV peak were taken from fit 1. Finally (fit 3), the region beginning with the 6.130-MeV single-escape peak and extending through the 7.117-MeV photopeak was fit with 34 variable parameters (24 amplitudes, eight 6.130-MeV peak positions, and two background parameters), where starting parameters for the 6.130-MeV peak were determined from Eq. (1) and those for the other two lines were taken from fit 2. The 6.917- and 7.117-MeV peak positions were fixed at the values obtained from fits 2 and 1, respectively. The final yields were taken from fit 3. There was no evidence in these fits for other γ rays in this region of the spectrum. A similar, but abbreviated, sequence was followed to extract 6.130- and 6.917-MeV γ-ray yields below 12 MeV α-particle energy, where there were no significant 7.117-MeV γ-ray yields.

C. Comparison of methods for peak area extraction

Of the two peak area extraction methods cited in Sec. II B, method B is the more reliable, but method A is considerably less laborious to apply and suffices when the peaks suffer relatively little Doppler broadening and when neighboring lines create no special problems. The two methods were used as follows: (a) Method B alone was used for the analysis of the (α,α') data from ^{12}C and ^{14}N at $E_\alpha > 16$ MeV and for the (α,α') data from ^{16}O at all incident energies; (b) method A was used for the (α,α') data from ^{12}C and ^{14}N at $E_\alpha < 16$ MeV, as corrected by spot checks using method B; and (c) method A alone was used for lines from reactions other than (α,α') reactions, because their cross sections are relatively small at the incident α-particle energies of the present measurements and they are of secondary interest.

For (b), the low-energy ^{12}C and ^{14}N data, the ratio of the counts found by the two methods was calculated at those incident energies where method B spot checks had been made. In most cases, the results of the two methods agreed to within better than ten percent, with the discrepancies smallest at low α-particle energies and increasing with E_α. Correction factors were determined from a linear best fit to the ratio as a function of E_α (for a given γ-ray line and detector), and the corrections were applied to the raw method A yields. With one exception, the largest correction was 9%. The exception was for the forward-angle data for the ^{14}N 1.635-MeV line, where a correction of up to 17% was required, traceable to difficulties created for the method A analysis by nearby lines from reactions in the nickel window of the gas cell.

III. RESULTS

A. General

The observed γ-ray yields all correspond to prompt reactions. Unlike the situation for proton-induced reactions (I), but just as in the case of α-particle-induced reactions on heavier nuclei (II), beta-delayed γ rays are unimportant in the present measurements. The $Z+1$ isobars of the residual nuclei being studied either cannot be produced at incident α-particle energies below 27 MeV or they decay with branching ratios of at least 99% to states that are too low in energy to contribute to the γ rays of interest.

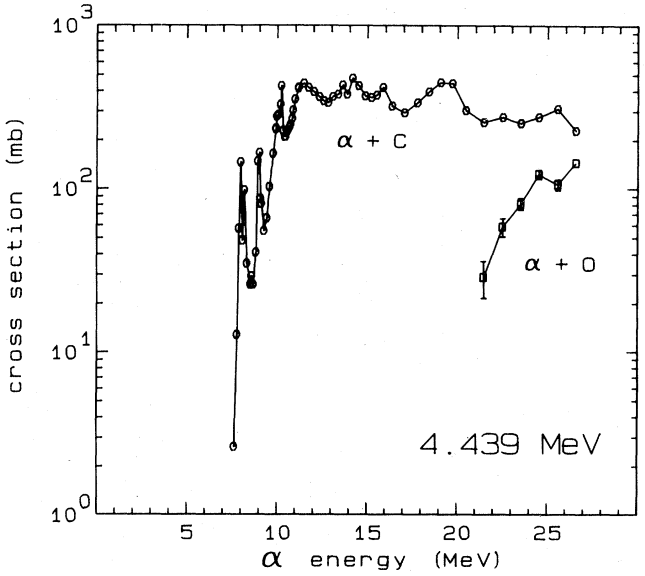

FIG. 3. Cross sections for the production of 4.439-MeV γ rays from the $\alpha+^{12}$C and $\alpha+^{16}$O reactions.

Results are presented in Figs. 3–5 as excitation function graphs and, in Table II, as a listing of cross sections averaged over bins of 1-MeV width, centered about the tabulated (target-center) laboratory energies.

Errors in the determination of absolute cross sections arise from errors in beam current integration (estimated at 3%), target thickness measurement (ranging from 5% to

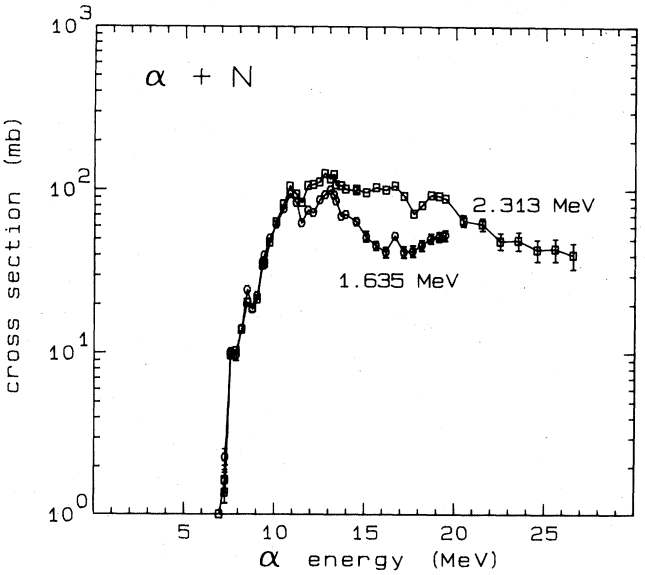

FIG. 4. Cross sections for the production of γ rays in (α,α') reactions on ^{14}N: the 1.635-MeV line from the (2-1) transition and the 2.313-MeV line from the (1-0) transition.

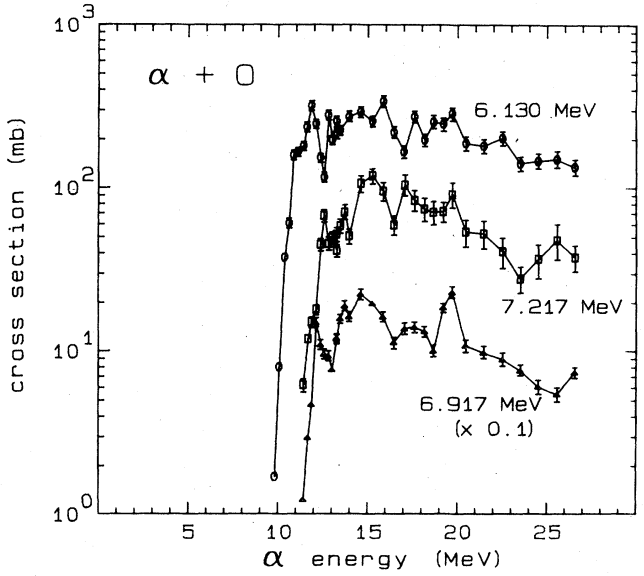

FIG. 5. Cross sections for the production of γ rays in (α,α') reactions on ^{16}O: the 6.130-MeV line from the (2-0) transition, the 6.917-MeV line from the (3-0) transition, and the 7.117-MeV line from the (4-0) transition. The 6.917-MeV excitation function has been shifted downward by a factor of 10 for clarity of display.

7%; see Table I), Ge(Li) efficiency measurement (estimated at 5% for low-energy γ rays, 10% for 4.439- and 6.130-MeV γ rays, and 15% for 6.917- and 7.117-MeV γ rays), and laboratory-to-center-of-mass conversions (estimated at 2%; see Sec. II A). Additional errors in determining peak yields, ranging from 5% to 27% (in cross section error), are discussed in Secs. III B—D. The errors quoted in Table II are derived from a quadratic sum of all the contributions. (Relative errors along a given excitation function are smaller.)

B. Carbon target

The most strongly excited γ-ray line in $\alpha+^{12}$C reactions is the 4.439-MeV line from the (1-0) (i.e., the first-excited-state to ground-state) transition in ^{12}C. The cross sections were determined from the photopeak yield, as described in Sec. II. They include a small subtraction, not exceeding 2 mb, for the contribution to the observed 4.439-MeV counts from the $(\alpha,2\alpha)$ reactions in the oxygen contaminant in the targets. The excitation function for the 4.439-MeV γ-ray yield is plotted in Fig. 3 and the cross sections are listed in Table II. Over a considerable energy interval, from $E_\alpha=11$ to 20 MeV, the cross section exceeds 300 mb. The relative uncertainties for individual points (not shown in the plot) range from 1% to 2%. They are statistical for $E_\alpha<19$ MeV. At higher energies, an error of 10% of the 5.241- plus 5.270-MeV yields has been included to account for possible systematic errors in unfolding these lines from the 4.439-MeV line. The errors quoted in Table II also include an overall 5% error to account for further systematic errors in yield extraction. The excitation function results are in agreement with the $(\alpha,\alpha'\gamma)$ results of Mitchell *et al.*[9] for $E_\alpha=6$ to 17 MeV, and the (α,α') results of Atneosen *et al.*[10] for $E_\alpha=20$ to 23 MeV, within errors.

Gamma rays from the ^{12}C$(\alpha,$p$)^{15}$N and ^{12}C$(\alpha,$n$)^{15}$O reactions are reasonably conspicuous in the spectrum. The combined cross sections for the 5.270-MeV (1-0) transition in ^{15}N and the 5.241-MeV (2-0) transition in ^{15}O be-

TABLE II. Cross sections (in mb) for the production of γ rays in α-particle-induced reactions. The cross sections are averages based on interpolation over 1-MeV wide bins centered at the indicated α-particle energies. Errors are derived from a quadratic sum of individual errors (see text).

Target	^{12}C	^{14}N	^{14}N	^{16}O	^{16}O	^{16}O	^{16}O
Residual	^{12}C	^{14}N	^{14}N	^{16}O	^{16}O	^{16}O	^{12}C
E (MeV)	4.439	1.635	2.313	6.130	6.917	7.117	4.439
E_α (MeV)							
8	48± 6	14±2	13± 1				
9	72± 9	27±3	25± 2				
10	231±30	61±5	62± 6	16± 2	1± 0.2		
11	347±45	83±7	95± 9	144±20	7±1		
12	393±51	76±8	105± 9	231±32	83±15	24± 4	
13	361±47	92±9	119±11	219±31	105±18	51± 9	
14	431±56	72±7	103± 9	269±38	183±31	62±11	
15	381±50	54±6	99±10	276±39	206±35	112±21	
16	371±48	45±5	102±10	288±43	149±25	85±18	
17	306±40	46±6	96±10	200±28	132±24	90±21	
18	361±47	45±6	79± 8	231±35	131±24	78±18	
19	435±57	52±8	92± 9	252±38	154±26	74±16	
20	382±53		76± 8	242±39	177±32	75±19	
21	276±39		64± 7	184±29	103±19	53±13	
22	265±37		56± 7	191±31	94±17	46±12	44±14
23	264±37		49± 7	170±27	83±15	34± 8	70±14
24	263±37		47± 8	143±23	69±12	32± 7	102±17
25	292±41		44± 8	148±24	58±11	42±11	114±19
26	272±38		42± 8	143±24	64±12	43±13	125±21

come significant above $E_\alpha = 19$ MeV, rising to about 50 mb at $E_\alpha = 20$ MeV and about 90 mb at $E_\alpha = 27$ MeV. Several lower-energy gamma rays from these two reactions are also visible in the spectra: at 1.885 and 2.297 MeV, from the (4-1) and (6-1) transitions in ^{15}N; and at 1.618 and 2.035 MeV, from the (5-2) and (6-2) transitions in ^{15}O. Of these, the 2.297-MeV yield is the highest over most of the beam-energy range. The threshold for producing this γ ray is $E_\alpha = 16.71$ MeV. At still higher energies, there is presumably also an unresolved contribution from the 2.313-MeV line from the (1-0) transition in ^{14}N, excited in the ^{12}C$(\alpha,\mathrm{d})^{14}$N reaction with a threshold at $E_\alpha = 21.18$ MeV. The cross section for this doublet does not exceed about 20 mb up to $E_\alpha = 26$ MeV. The doublet is observable in the $\alpha + ^{12}$C spectrum, despite the low cross section, in part because there are no (α,α') lines in the region and in part because there is little Doppler broadening for an (α,p) reaction near threshold. However, it is unlikely that it could be seen in an astrophysical observation, unless the cross section rises unexpectedly at higher energies.

C. Nitrogen target

Over most of the incident energy range of the present experiment, the most prominent lines in the $\alpha + ^{14}$N spectrum are those excited in (α,α') reactions: the 1.635-MeV line from the (2-1) transition and the 2.313-MeV line from the (1-0) transition. The excitation functions for producing these lines are plotted in Fig. 4 and the cross sections listed in Table II. For the 1.635-MeV line, results are presented only up to $E_\alpha = 19.5$ MeV, because above this energy the peak in the spectrum was not well enough defined for reliable peak area extraction.

Only statistical errors are included in the error bars of Fig. 4 for the 2.313-MeV line at $E_\alpha < 21$ MeV and for the 1.635-MeV line. Above 21 MeV, where the peak-to-background ratios were low, additional errors ranging from 5% to 18% have been included for the 2.313-MeV line, to account for systematic errors in fitting spectra. The errors quoted in Table II include these errors as well as the errors discussed in Sec. III A. They also include: (a) 5% errors in peak extraction for the 2.313-MeV line for $E_\alpha < 21$ MeV and for the 1.635-MeV line; and (b) an additional error arising from the nickel-window background subtraction for the 1.635-MeV line above $E_\alpha = 15$ MeV (see Sec. II). This last term, derived by assigning a 50% error to the number of Ni counts subtracted, corresponds to a contribution of 5% to 9% to the cross section error.

It is seen that at low energies the cross sections for the two lines are the same, within experimental uncertainties, while above $E_\alpha = 10$ MeV the 2.313-MeV yield clearly exceeds the 1.635-MeV yield. This is to be expected, because the (α,α') reaction to the 2.313-MeV first excited state is isospin forbidden, and the third excited state at 4.915 MeV decays almost entirely to the ground state. Thus, the 2.313-MeV yield cannot significantly exceed the 1.635-MeV yield, until the state at 5.106 MeV (the fourth excited state with a 19% branching ratio to the 2.313 MeV state) is reached.

The maximum cross section for the 2.313-MeV line, about 130 mb near 12 MeV, is only about one-third of the maximum reached for the 4.439-MeV line from the ^{12}C$(\alpha,\alpha')^{12}$C reaction. The lower cross sections, coupled with the comparatively low abundance of nitrogen in standard environments (the solar system abundance is about 20% that of carbon[11]), make it unlikely that the 2.313-MeV line will be conspicuous in astrophysical observations. Conversely, a relatively strong 2.313-MeV line would suggest an unusually high ^{14}N abundance. The 1.635-MeV γ rays from ^{14}N will contribute to the overall magnitude of a multiplet which also includes a contribution from the 1.634-MeV line in ^{20}Ne, excited in the (α,α') reaction on ^{20}Ne and in the $(\alpha,2\alpha)$ reaction on ^{24}Mg.

Alpha-particle interactions with ^{14}N can also contribute to the production of the 6.130-MeV line of ^{16}O, through the ^{14}N$(\alpha,\mathrm{d})^{16}$O reaction, with a threshold at $E_\alpha = 11.88$ MeV. However, the cross section for this line was not investigated in detail because normally the abundance of ^{16}O is substantially greater than that of ^{14}N, e.g., a factor of 10 greater for the solar system abundances.[11] In a determination at one energy and angle, $E_\alpha = 24$ MeV and $\theta = 90°$, the 6.130-MeV γ-ray cross section was found to be about 6 mb/sr, corresponding to a total cross section in the neighborhood of 75 mb if the angular distribution is not too far from isotropic. For the (α,α') reaction on ^{16}O at this energy, the total cross section is about 140 mb. Thus, in most anticipated environments nitrogen will make little contribution to the total yield of 6.130-MeV γ rays.

D. Oxygen target

Cross sections were determined for three lines in ^{16}O from (α,α') reactions: the 6.130-, 6.917- and 7.117-MeV lines, corresponding to the (2-0), (3-0), and (4-0) transitions. The total cross section for the 6.130-MeV γ rays, for which $l_{\max} = 6$ in a Legendre polynomial expansion of the angular distribution, was found explicitly from the counts at four angles. For the remaining lines, as well as for the 4.439-MeV line from ^{12}C (see below), the total cross sections were determined from a Legendre polynomial best fit to data at four angles (26°, 48.8°, 90°, and 104°), using the standard program, LEGFIT (Ref. 12) with $l_{\max} = 4$.

The excitation functions for these lines are plotted in Fig. 5 and the cross sections are listed in Table II. Error bars shown on the excitation function plot are primarily systematic, and are derived from an attempt to account for unfolding errors in the yield extraction technique by considering the consistency of angular distributions, fluctuations in the ratio of counts in the two detectors, the dependence of results on the starting parameters in spectrum fitting, and the relative strengths of the lines in the spectrum. These errors are included in the errors quoted in Table II. Our cross sections for 6.130-MeV γ rays are about half those inferred from the results of Mehta *et al.*[13] for $E_\alpha = 11$–17 MeV which we estimated by multiplying the reported 0° differential cross section by 4π. Agreement is better for $E_\alpha = 17$–19 MeV. As the absolute cross section error quoted by Mehta *et al.* is $\pm 45\%$, and there are uncertainties of the order of 30% in deducing

the total cross section from results at one angle, the discrepancies are not outside errors.

At the higher energies, there is also an appreciable yield for the 4.439-MeV line of ^{12}C, produced in the $(\alpha,2\alpha)$ reaction. The excitation function is plotted in Fig. 3, along with the excitation function for producing 4.439-MeV γ rays in the (α,α') reaction on ^{12}C. The errors in the figure are statistical only. Those of Table II include these statistical errors plus an estimated 10% systematic error in peak extraction. The cross section rises rapidly above $E_\alpha=21$ MeV, but even for our highest energy point, centered at 26.5 MeV, the $(\alpha,2\alpha)$ cross section is less than the (α,α') cross section. Nevertheless, given the high abundance of oxygen (e.g., a $^{16}O/^{12}C$ abundance ratio of 1.7),[11] the $(\alpha,2\alpha)$ contribution may be important in some situations.

Unlike the case of heavier targets (II), and even ^{12}C, lines from (α,p) and (α,n) reactions are found to be only weakly excited in $\alpha+^{16}O$ interactions. The most prominent such lines in our spectra are the poorly resolved doublet made up of the 2.583-MeV line from the (6-2) transition in ^{19}F and the 2.557-MeV line from the (6-1) transition in ^{19}Ne, with thresholds at $E_\alpha=13.62$ and 18.67 MeV, respectively. The combined cross section at $E_\alpha=24$ MeV is in the neighborhood of 30 mb. With so small a cross section, it appears unlikely that this doublet will be readily observable in astronomical spectra, despite the high oxygen abundance.

IV. DISCUSSION

Lines from inelastic scattering reactions dominate the γ-ray spectra in the present data more markedly than they do either for proton-induced reactions (I) or for α-particle induced reactions on heavier nuclei (II), where, for example, $(p,p\alpha)$ or (α,p) lines are strongly excited. Thus, the only prominent $(\alpha,2\alpha)$ line is the 4.439-MeV line produced in the $^{16}O(\alpha,2\alpha)^{12}C$ reaction, and even here the $(\alpha,2\alpha)$ cross section remains lower than the (α,α') cross section for all measured energies. Similarly, the yields for (α,p) and (α,n) reactions are less prominent for ^{12}C, ^{14}N, and ^{16}O than had been the case for intermediate mass targets (II).

It was pointed out in (II) that the rapid drop in cosmic isotopic abundances with increasing mass number above $A=56$, combined with the high cross sections for (α,n) and (α,p) reactions in intermediate mass nuclei, means that the observation of lines from $A=58$ or 59 nuclei excited in $\alpha+^{56}Fe$ reactions could serve as a diagnostic for high α-particle fluxes. Although there is also a drop in cosmic abundances above ^{16}O, the relevant cross sections were found to be too small to make such an approach promising using lines from $\alpha+^{16}O$ reactions (see Sec. III D).

The relative observability in astronomical spectra of γ-ray lines from α-particle-induced and proton-induced reactions is determined by the relative magnitudes of the cross sections, the relative particle fluxes at energies where the cross sections are high, and the relative widths of the lines. Although in normal environments it is expected that total proton fluxes are substantially greater than total α-particle fluxes, it is less clear that the proton-to-alpha-particle flux ratio is high at low kinetic energies (e.g., comparing 10-MeV protons where $E/A=10$ MeV/nucleon to 10-MeV α particles where $E/A=2.5$ MeV per nucleon). Thus, as discussed in (II), the expected systematic favoring of proton-induced reactions may not be very great, especially in environments where the energy spectra rise rapidly with decreasing energy.

An unambiguous disadvantage of α-particle-induced reactions, in terms of γ-ray observability, is the greater Doppler broadening, which is particularly significant for the light targets studied in the present paper. For example, the recoiling excited ^{12}C nuclei have a maximum velocity of $\beta=0.053$ for 24-MeV incident α particles and of $\beta=0.033$ for 24-MeV incident protons. Thus the kinematic limits on the width of the 4.439-MeV ^{12}C line, for extreme forward and backward γ rays, are about 0.47 MeV for α particles and 0.30 MeV for protons. While the Doppler broadening will make it more difficult to observe the lines above background, the line width in principle offers a way to distinguish between incident α particles and protons.

From the results reported for α particles in Sec. III and for protons in a previous paper (I), it is seen that in general the magnitudes of the (α,α') cross sections are greater than those for the (p,p') cross sections for the most conspicuous lines. Thus, for the 6.130-MeV line from ^{16}O, the maximum (α,α') cross section is about 300 mb (near $E_\alpha=16$ MeV) while the maximum (p,p') cross section is only about 160 mb (near $E_p=13$ MeV). For the 4.439-MeV line from ^{12}C, the cross sections are both in the neighborhood of 300 mb near 10 MeV, but the (p,p') cross section peaks near $E_p=11$ MeV and drops to 125 mb at 20 MeV, while the (α,α') cross section stays above 300 mb for almost the entire region between $E_\alpha=10$ and 20 MeV. The cross sections for the 2.313-MeV line from ^{14}N are in both cases relatively low, but again the (α,α') cross sections are the larger except at low energies.

In view of typical cosmic abundances and of the relative magnitudes of the cross sections, the largest γ-ray fluxes for α-particle-induced reactions can be expected to be those from the 4.439- and 6.130-MeV lines produced in inelastic scattering. Whether these will indeed be conspicuous when compared to the same lines from (p,p') scattering will depend on the relative magnitudes and energy spectra of the particle fluxes.

---

*Present address: Los Alamos National Laboratory, Physics Division, MS D449, Los Alamos, NM 87545.

†Present address: Nuclear Science Division, Lawrence Berkeley Laboratory, Berkeley, CA 94720.

‡Present address: John Fluke Manufacturing Co., MS 281H, Everett, WA 98206.

[1]R. Ramaty and R. E. Lingenfelter, Annu. Rev. Nucl. Part. Sci. **32**, 235 (1982); Space Sci. Rev. **36**, 305 (1983).

[2]E. L. Chupp, Annu. Rev. Astron. Astrophys. **22**, 359 (1984).

[3]C. J. MacCallum and M. Leventhal, *Position-Electron Pairs in*

Astrophysics (Goddard Space Flight Center, 1983), AIP Conf. Proc. No. 101, edited by M. L. Burns, A. K. Harding, and R. Ramaty (AIP, New York, 1983), p. 211.

[4]R. C. Lamb, J. C. Ling, W. A. Maloney, G. R. Riegler, W. A. Wheaton, and A. S. Jacobson, Nature **305**, 37 (1983).

[5]P. Dyer, D. Bodansky, A. G. Seamster, E. B. Norman, and D. R. Maxson, Phys. Rev. C **23**, 1865 (1981).

[6]A. G. Seamster, E. B. Norman, D. D. Leach, P. Dyer, and D. Bodansky, Phys. Rev. C **29**, 394 (1984).

[7]B. W. Sargent and A. Henrikson, Nucl. Instrum. Methods **189**, 459 (1981).

[8]J. J. Kolata, R. Auble, and A. Galonsky, Phys. Rev. **162**, 957 (1967).

[9]G. E. Mitchell, E. B. Carter, and R. H. Davis, Phys. Rev. **133**, B1434 (1964).

[10]R. A. Atneosen, H. L. Wilson, M. B. Sampson, and D. W. Miller, Phys. Rev. **135**, B660 (1964).

[11]A. G. W. Cameron, in *Essays in Nuclear Astrophysics,* edited by C. A. Barnes, D. D. Clayton, and D. N. Schramm (Cambridge University Press, Cambridge, 1982), p. 23.

[12]Philip R. Bevington, *Data Reduction and Error Analysis for the Physical Sciences* (McGraw-Hill, New York, 1969).

[13]M. K. Mehta, W. E. Hunt, and R. H. Davis, Phys. Rev. **160**, 791 (1967).